Process Systems Engineering and Process Safety

Fault detection of large-scale process control system with higher-order statistical and interpretative structural model ☆

Zhiqiang Geng [1], Ke Yang [1], Yongming Han [1], Xiangbai Gu [1,2,*]

[1] College of Information Science and Technology, Beijing University of Chemical Technology, Beijing 100029, China
[2] Sinopec Engineering (Group) Co., Ltd., Beijing 100101,China

ABSTRACT

Nonlinear characteristic fault detection and diagnosis method based on higher-order statistical (HOS) is an effective data-driven method, but the calculation costs much for a large-scale process control system. An HOS-ISM fault diagnosis framework combining interpretative structural model (ISM) and HOS is proposed: (1) the adjacency matrix is determined by partial correlation coefficient; (2) the modified adjacency matrix is defined by directed graph with prior knowledge of process piping and instrument diagram; (3) interpretative structural for large-scale process control system is built by this ISM method; and (4) non-Gaussianity index, nonlinearity index, and total nonlinearity index are calculated dynamically based on interpretative structural to effectively eliminate uncertainty of the nonlinear characteristic diagnostic method with reasonable sampling period and data window. The proposed HOS-ISM fault diagnosis framework is verified by the Tennessee Eastman process and presents improvement for highly non-linear characteristic for selected fault cases.

© 2014 The Chemical Industry and Engineering Society of China, and Chemical Industry Press. All rights reserved.

1. Introduction

With the development of industrial automation and integration, improvement of fault diagnosis technology has a great significance for industry. Recently, the development of computer and signal processing technologies promotes the development of fault diagnosis technology. Fault diagnosis methods can be divided into knowledge approach, analytical model approach and signal processing approach. Venkatasubramanian et al. [1–3] have divided diagnostic methods into quantitative model method, qualitative model method and historical data method. Some methods have been proposed based on data-driven diagnostic, such as principal component analysis (PCA), kernel principal component analysis (KPCA) [4,5], fisher discriminant analysis [6], and others using AI in fault diagnosis [7–9]. New theories are introduced to fault diagnosis, such as model reasoning methods based on graph theory and methods with evolutionary algorithm [10].

HOS is one of the data-driven methods. Third-order and fourth-order moments or higher order statistics are used for nonlinear analysis on communication signal, radar signal, nonlinear seismic wave and audio signal and monitoring mechanical condition [11–13]. Choudhury

et al. [14] first proposed non-Gaussianity index (NGI) and nonlinearity index (NLI), and applied the index to nonlinear characteristic diagnostic of control loops successfully. Choudhury [15] modified NGI and NLI and proposed a new index, total nonlinearity index (TNLI), to measure the degree of nonlinearity, with the diagnostic rate of false positives reduced. These indices have been used to detect the valve adhesion and poor controller performance. However, the difference of data selection causes inconclusive results, lowering the efficiency of nonlinear characteristics of the diagnosis. Besides, bicoherence is so sensitive that the indexes will change a lot if the data have any change. For complex and multi-variable systems, it is necessary to improve the method due to unclear goals of higher-order statistics.

In 1973, ISM was developed by J. Warfield to analyze complex systems. Recently, Peng applied it on the outline design stage [16]. Wang et al. applied it to analyze the cause of accident level [17]. Yang et al. investigated the effect of workplace risk by combining ISM and hierarchical approach [18]. Singh and Kant made use of ISM to determine the relationship among the knowledge management barriers [19]. However, the adjacency matrix is mostly established with the knowledge of expert system, which has the disadvantage of great subjectivity and inconsistency. Data-driven methods without prior knowledge also have the disadvantage of great blindness. Hence, establishment of adjacency matrix of ISM needs to combine prior knowledge and a data-driven method based on partial correlation coefficient. In other words, both methods can authenticate and compensate each other. Yan [20] established online contacts between two variables with comparing partial correlation coefficient and correlation coefficient. Wang et al. [21]

considered that partial correlation coefficient is more effective with independent variables. Kim *e al.* [22] studied Copula function modeling using partial correlation coefficient. Yang *et al.* used correlation coefficient method to verify the efficiency of signed directed graph model [23].

ISM can be used to improve the efficiency of the method and diagnostic purposes in this study. This paper describes the relation between variables using partial correlation coefficients for defining the adjacency matrix, modifies this adjacency matrix based on priori knowledge of process piping and instrument diagram, and builds ISM of control loop system. Then above structural information is integrated with nonlinear characteristic diagnostic method, which is based on higher-order statistical, for more effective diagnosis of nonlinear characteristic of process.

2. Interpretative Structural for Control System Based on ISM

The correlation coefficient describes the relationship among variables and it is seldom used to infer the inner relationship of variables. Whether the relationship is related with other factors, it should be considered. The partial correlation coefficient measures the ceteris paribus effect among variables and reflects the real linkage of variables, and as the strength of the relationship between variables increases, the absolute value of partial correlation coefficient also increases. Because of the influence of ceteris paribus, the correlation between dependent and independent variables is a dimensionless number between -1 and 1. We usually use its absolute value.

2.1. Modeling of partial correlation coefficient matrix

The normal data of all control loops are chosen and normalized as:

$$x_{ij} = \frac{x_{ij} - x_j^{min}}{x_j^{max} - x_j^{min}} \tag{1}$$

where

$$x_j^{min} = \min\left\{x_{1j}, x_{2j}, \cdots x_{tj}\right\}, j = 1, 2, \cdots t$$

$$x_j^{max} = \max\left\{x_{1j}, x_{2j}, \cdots x_{tj}\right\}, j = 1, 2, \cdots m,$$

t is the number of control loops and m is the number of samples with value of 500 in this paper. According to experimental verification, Outputs of control loops are used, which describe the relationship of control loops better.

Let $x_i(i = 1, 2, \ldots, m)$ be the i-th value of variable x, then the correlation coefficient of x_i and y_i is

$$r_{xy} = \frac{\sum_{i=1}^{M}(x_i - \overline{x})\left(y_j - \overline{y}\right)}{\sqrt{\sum_{i=1}^{M}(x_i - \overline{x})^2}\sqrt{\sum_{i=1}^{M}(y_i - \overline{y})^2}} \tag{2}$$

where $\overline{x}$ is the mean value of x_i, and $\overline{y}$ is the mean value of y_i.

From the Eq. (1), we can get the correlation coefficient matrix

$$r = \begin{bmatrix} r_{11} & r_{12} & \cdots & r_{1n-1} & r_{1n} \\ r_{21} & r_{22} & \cdots & r_{2n-1} & r_{2n} \\ & & \cdots\cdots\cdots\cdots & & \\ r_{m1} & r_{m2} & \cdots & r_{m-1n-1} & r_{mn} \end{bmatrix}_{m \times n}. \tag{3}$$

The correlation coefficient matrix is computed and the inverse matrix is obtained, which is used to obtain the partial correlation coefficient matrix.

The inverse matrix of r is

$$c = \text{inv}(r) = \begin{bmatrix} c_{11} & c_{12} & \cdots & c_{1n-1} & c_{1n} \\ c_{21} & c_{22} & \cdots & c_{2n-1} & c_{2n} \\ & & \cdots\cdots\cdots\cdots & & \\ c_{m1} & c_{m2} & \cdots & c_{m-1n-1} & c_{mn} \end{bmatrix}_{m \times n}. \tag{4}$$

Then the partial correlation coefficient of the two variables is

$$R_{ij} = -\frac{c_{ij}}{\sqrt{c_{ii} * c_{jj}}} \tag{5}$$

where $i = 1, 2, \ldots, m$ and $j = 1, 2, \ldots, n$.

And

$$R = \begin{bmatrix} R_{11} & R_{12} & \cdots & R_{1\ n-1} & R_{1\ n} \\ R_{21} & R_{22} & \cdots & R_{2\ n-1} & R_{2\ n} \\ \cdots & \cdots & \cdots & \cdots & \cdots \\ R_{n2} & R_{n2} & \cdots & R_{n\ n-1} & R_{n\ n} \end{bmatrix}. \tag{6}$$

There are different definitions in different industries whether the partial correlation coefficient is related. Table 1 shows the general scope of partial correlation coefficient.

Table 1
The scope of partial correlation coefficient

Scope of partial correlation coefficient	Relationship
$0 \le |R_{ij}| < 0.1$	No
$0.1 \le |R_{ij}| < 0.3$	Low
$0.3 \le |R_{ij}| < 0.5$	Medium
$0.5 \le |R_{ij}| < 0.8$	Strong
$0.8 \le |R_{ij}| < 1$	Extremely strong

2.2. Interpretative structural model with priori knowledge of PID

If R_{ij} is a positive number and greater than the threshold value, then $a_{ij} = 1$ and $a_{ij} = 0$ where a_{ij} is the adjacency value of x_i to x_j, otherwise, $a_{ij} = 0$ and $a_{ij} = 1$. The adjacency matrix is

$$A = \begin{bmatrix} a_{11} & a_{12} & \cdots & a_{1\ n-1} & a_{1\ n} \\ a_{21} & a_{22} & \cdots & a_{2\ n-1} & a_{2\ n} \\ \cdots & \cdots & \cdots & \cdots & \cdots \\ a_{n2} & a_{n2} & \cdots & a_{n\ n-1} & a_{n\ n} \end{bmatrix} \tag{7}$$

where $a_{ij} = 1$ or $a_{ij} = 0$ ($i = 1, 2, \ldots, n; j = 1, 2, \ldots, n$).

Modifying adjacency matrix A', we can build the control loop directed graph. The relationship of control loops is described by priori knowledge of piping and instrument diagram (PID) [24] in process flow chart. Adjacency matrix A is modified by the control loop directed graph. For instance, if node-i has an effect on node-j or node-i → node-j in process flow chart, the value of a_{ij} is set to 1, or $a_{ij} = 0$ in adjacency matrix A. Both methods can authenticate and compensate each other. Finally, adjacency matrix A' is finished.

With the $n \times n$ identity matrix

$$E = \begin{bmatrix} 1 & 0 & \cdots & 0 & 0 \\ 0 & 1 & \cdots & 0 & 0 \\ \cdots & \cdots & \cdots & \cdots & \cdots \\ 0 & 0 & \cdots & 0 & 1 \end{bmatrix} \tag{8}$$

we have

$$A' + E = (A' + E)^2 = \cdots = (A' + E)^{n-1} = (A' + E)^n. \tag{9}$$

We can get formula $\mathbf{RE} = (\mathbf{A}' + \mathbf{E})^{n-1}$, which is the reachability matrix of adjacency matrix $\mathbf{A}'$

$$\mathbf{RE} = \begin{bmatrix} RE_{11} & RE_{12} & \cdots & RE_{1n-1} & RE_{1n} \\ RE_{21} & RE_{22} & \cdots & RE_{2n-1} & RE_{2n} \\ \cdots & \cdots & \cdots & \cdots & \cdots \\ RE_{n2} & RE_{n2} & \cdots & RE_{n\ n-1} & RE_{nn} \end{bmatrix}. \quad (10)$$

Definition 1. In the i-th row RE_i ($i = 1, 2, ..., n$) of reachability matrix $\mathbf{RE}$, if $RE_{ij} = 1$ ($j = 1, 2, ..., n$), then element RE_{ij} is added to the reachable set, which is expressed as S_i.

Definition 2. In the j-th column RE_j ($j = 1, 2, ..., n.$) of reachability matrix $\mathbf{RE}$, if $RE_{ij} = 1$ ($i = 1, 2, ..., n$), then element RE_{ij} is added to the first set, which is expressed as B_j.

The influencing factors can be stratified based on $S_i \cap B_j = S_i$, and then the highest level of factors L_1 is identified. The column and the row corresponding with L_1 are removed from the reachability matrix $\mathbf{RE}$. By the same decision rules, $L_2, L_3 ..., L_k$ are definite. The last step is to model the hierarchy of ISM using each level of L. Specific examples are shown in Section 4.

The detail steps for this algorithm are described in the ISM framework in Section 3.2. According to the ISM, a control loop system is divided into several small sets of control loops, which are used to systematic fault detection and diagnosis. This method avoids the blindness of diagnosis and increases diagnostic efficiency.

3. HOS–ISM Fault Diagnosis Framework

In practice, many industrial processes include not only Gaussian signals but also non-Gaussian and nonlinear signals, which cannot be identified by the first order and second order signals. Higher-orderstatistical theory is a good choice for identifying these signals. The method of non-linearity detection uses HOS because it is sensitive to certain types of phase coupling between different frequency bands [25].

3.1. Indexes of HOS

Non-Gaussianity index and nonlinearity index are based on the statistical hypothesis test [14]. The principal domain of the bicoherence is $0 < f_1 < 0.5, f_2 < f_1$ and $2f_1 + f_2 < 1$. Then they are modified and TNLI is proposed [15].

Non-Gaussianity index is defined as:

$$NGI \triangleq \frac{\sum bic^2_{significant}}{L} - \frac{c^{\chi^2}_\alpha}{2K} \quad (11)$$

where $bic^2_{significant}$ presents the bicoherence that fails the hypothesis test, K is the number of data segments, and $c^{\chi^2}_\alpha$ is the critical value calculated from the central χ^2 significance level of α at degrees of freedom 2. Unless otherwise stated, $\alpha = 0.05$ and $c^{\chi^2}_\alpha = 5.99$ [8].

Nonlinearity Index is defined as

$$NLI \triangleq bic^2_{max} - \left(\overline{bic^2_{robust}} + 2\sigma_{bic^2,\ robust} \right) \quad (12)$$

where $\overline{bic^2_{robust}}$ and $\sigma_{bic^2,\ robust}$ are the robust mean and the robust standard deviation of the estimated squared bicoherence [8].

Total nonlinearity index is defined as

$$TNLI \triangleq \sum bic^2_{significant}. \quad (13)$$

It is an important index to compare the extent of nonlinearities. Fig. 1 is the rule based decision flow diagram by nonlinearity indexes [14], where $\alpha = 0.05$. After the fault occurs, it can be used to feature
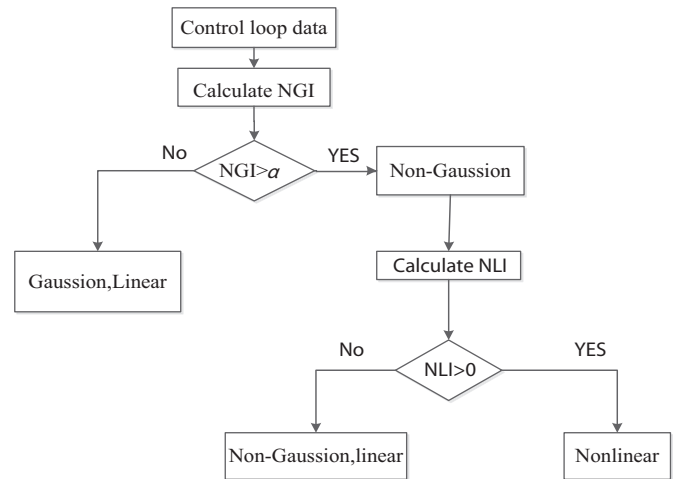
Fig. 1. Rule based decision flow diagram.

extraction of fault. The calculation is based on data length of 4096, segment length of 64, 50% overlap, Hanning window with length of 64, and DFT length of 128 for one index of HOS[14].

3.2. Fault diagnosis framework based on HOS–ISM

The indexes are applied in a new way with moving window in this paper. Since the calculation of these indexes is based on data, different data will lead to uncertain results of diagnosis. There are a lot of day-to-day monitoring and operation data in industrial processes. Section 3.1 only shows a handful of index calculation without the variation of indexes. The dynamic calculation for these indexes is needed. The proposed fault detection and diagnosis framework is showed in Fig. 2.

The framework includes online and offline parts. The goal of offline is to build ISM of control loop system. For online part, after data collection, choose a small loop set by the graph based on ISM, then extract nonlinear feature and judge the fault. Specific example will be given in Section 4.

This framework process is as follows.

Step 1 Build interpretative structural model (Section 2).
Step 2 Obtain data collection from process with a fault.
Step 3 Choose data in small loop set (level i) using ISM of control system. When the fault is not detected, the small control loop set in lower level ($i - 1$) is selected. The level is chosen from the bottom level to the upper level. These sets are good for fault detection and diagnosis order in this framework.
Step 4 Dynamically extract nonlinear feature by calculating TNLI,NGI and NLI.
        We selected data by moving window with a length of 4096 at a step of 64 and searching the index variation. Meanwhile, moving window is used to implement indexes of HOS in on-line manner, where the window length is maintained by introducing the most recent measurement and discarding the oldest one. In other words, one index calculation needs 4096 data length and dynamical calculation needs a moving window with a length of 4096. PV-SP of every control loop is used to calculate three indexes [15]. NGI and NLI are calculated as shown in Fig. 1 and TNLI can be calculated.
Step 5 Fault is detected according to nonlinear feature from Step 4. After comparison to the nonlinear feature of control loops, if fault is detected, this process will be recovered. Otherwise, go back to Step 3.
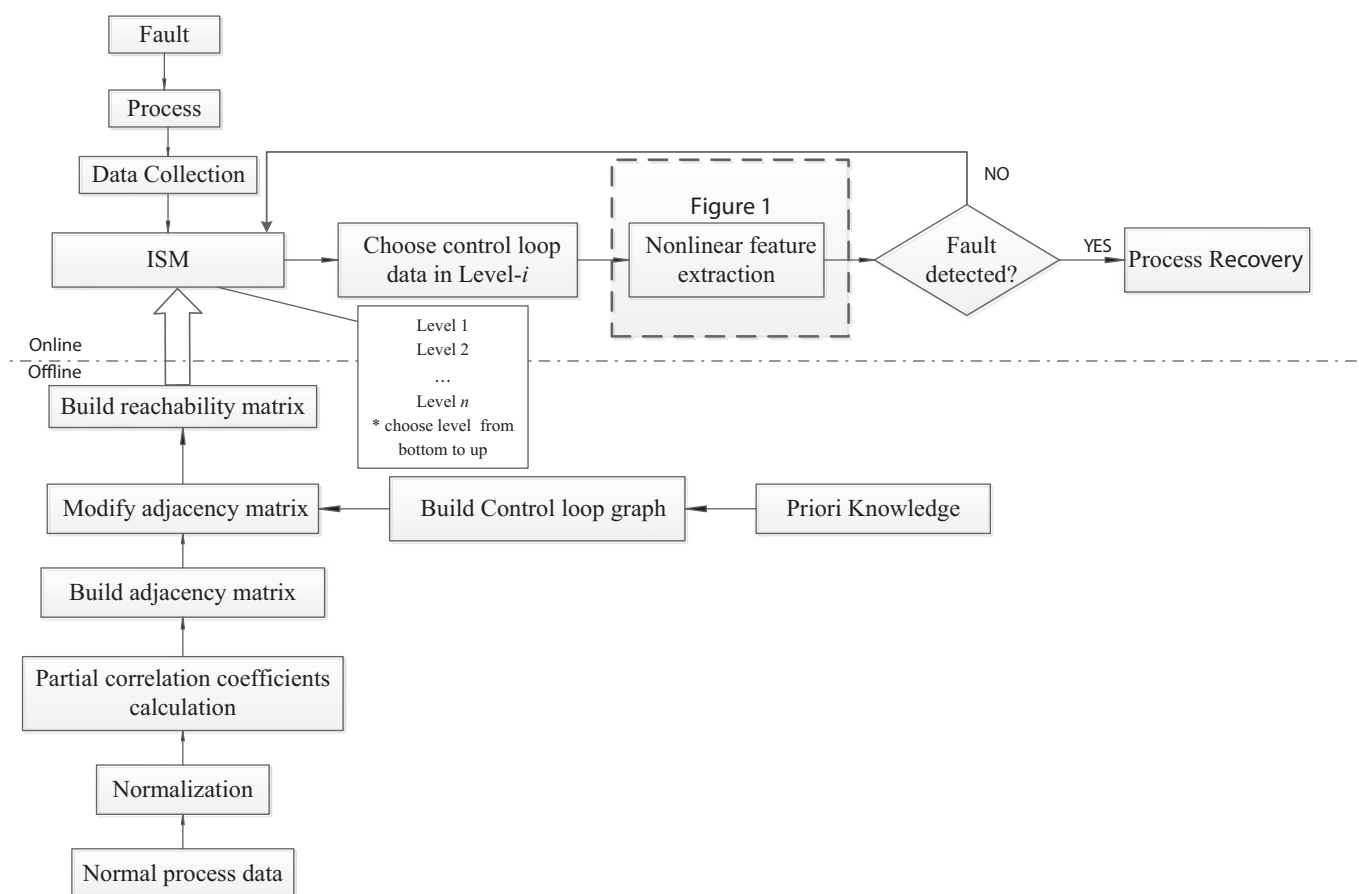
Fig. 2. The proposed fault detection and diagnosis framework.

4. Cases of the Tennessee Eastman Process

4.1. Tennessee Eastman process

The Tennessee Eastman (TE) process is a classic chemical process simulation model proposed by Downs and Vogel [26]. It is usually used to multivariable control, nonlinear control, optimization, model predictive control and fault diagnosis [27–29]. TE process includes reactor, condenser, compressor, vapor/liquid separator and stripper, with 41 measurements containing 22 continuous variables and 19 chromatography component measurement values and with 12 manipulated variables and 20 disturbances which can be set [30].

4.2. Building ISM of TE process

Larsson [31] has proposed a self-optimizing control of TE process and simulated it with Matlab. Here we paper use a model named MultiLoop_Skoge_mode1 in Matlab for getting data of TE process. Control loops of TE are analyzed in Table 2 where r1, r2, r3, r4, r5, r6, r7, FP, SP17, PctGsp, and Eadj are intermediate variables of TE process, which are useful for calculation. For getting real-time data of these intermediate variables, TE simulation is modified without affecting the operation. A control loop digraph can be built by *a priori* knowledge, as shown in Fig. 3.

The simulation data of TE process without disturbances are obtained. According to the ISM framework in Fig. 2, adjacency matrix (Table 3), modified adjacency matrix (Table 4), and reachability matrix (Table 5) can be finished, and ISM is built (Table 6). Control loops of Level 7

present the highest influence on control system and the impact of the front level is weak. The small control loop sets in Table 6 are good for an effective fault detection and diagnosis of HOS.

4.3. Nonlinear characteristic analysis based on HOS

The above description shows the importance and relation of control loops in TE process. It is helpful to the next nonlinear characteristic

Table 2
Control loops of TE control process

Number of control loop	SP	PV	O P
1	r1*FP	XMEAS1	XMV3
2	r2*FP	XMEAS2	XMV1
3	r3*FP	XMEAS3	XMV2
4	r4*FP	XMEAS4	XMV4
5	Reactor level SP = 65	XMEAS8	sp17
6	Reactor pressure SP = 2800	XMEAS7	r5
7	Reactor temperature SP = 122.9	XMEAS9	xmv10
8	SP17	XMEAS11	xmv11
9	C in purge SP = 13.1%	XMEAS31	r4
10	Separator level SP = 50	XMEAS12	r6
11	r6*FP	XMEAS14	XMV7
12	Stripper level SP = 50	XMEAS15	r7
13	r7*FP	XMEAS17	XMV8
14	r5*FP	XMEAS10	XMV6
15	G in product =53.8%	XMEAS40	Eadj
16	Product SP = 22.89	XMEAS17	FP
17	Separator underflow SP = 32.2	XMEAS5	r1

Fig. 3. Control loop digraph of TE process.

analysis. A dynamic calculation is introduced into NLI,TNLI and NGI in the following four cases, and the dynamic figure is obtained, with which the location and point of failure can be identified. This study concentrates on those faults that produce large impact and occur at control loops. Three cases IDV(4), IDV(11) and IDV(14), with different interfering signals and same location, are chosen for studying characters of these indexes. Case IDV(12) occurs at other loop.

4.3.1. Case 1—IDV(4)

After running TE simulation model, IDV(4) (pulse), associated with step change in the reactor cooling water inlet temperature, is set to

pulse interference at 71 h. PV-SP of each loop is acquired, values of NLI, TNLI and NGI are calculated with 64 steps interval. With small control loop set (Table 6), these indexes can be calculated. The fault is not detected until control loops in Level 2 are chosen.

Fig. 4 shows that the curves of loop 7 are very similar and the process experiences steady state, sudden rise, and fall to ultimate stability, due to pulse signal.

For NLI, it has step change when the fault signal enters into the window of 4096, so its value increases suddenly; it keeps relatively stable as the fault signal moves along the window of 4096 and falls suddenly when the fault signal moves out of the window. It is easy to determine

Table 3
Adjacency matrix **A** of TE process based on partial correlation coefficient

	1	2	3	4	5	6	7	8	9	10	11	12	13	14	15	16	17
1	1	1	1	1	1	0	1	0	0	1	1	1	0	0	0	1	0	0
2	0	1	1	0	0	1	0	0	0	0	0	0	0	0	0	0	0
3	0	0	1	0	0	0	0	0	0	1	0	0	0	0	0	0	0
4	0	0	1	1	0	1	0	0	1	0	0	0	0	0	1	0	0
5	0	0	0	0	1	0	0	0	0	0	1	0	0	0	0	0	0
6	0	0	0	0	0	1	0	0	0	0	0	0	0	0	0	0	0
7	0	0	0	0	0	1	1	1	0	0	0	0	0	0	0	0	0
8	0	0	0	0	0	1	0	1	0	0	0	0	0	0	0	0	0
9	0	0	0	1	0	1	0	0	1	0	0	0	0	0	0	0	0
10	0	0	0	0	0	0	0	0	0	1	0	0	0	0	0	0	0
11	0	1	1	0	0	0	0	0	0	0	1	1	0	1	0	0	0
12	0	0	0	0	0	0	0	0	0	0	0	1	0	0	0	0	0
13	0	1	1	0	0	1	0	0	0	0	0	0	1	0	1	0	0
14	0	1	1	1	0	1	1	0	1	0	0	0	1	1	1	0	0
15	0	1	1	0	0	0	0	0	0	0	0	0	0	0	1	0	0
16	0	0	0	0	0	0	0	0	0	0	0	0	0	1	1	0
17	0	0	0	0	0	0	0	0	0	0	0	0	0	0	0	1

Table 4
Modified adjacency matrix **A**′ of TE process

	1	2	3	4	5	6	7	8	9	10	11	12	13	14	15	16	17
1	1	1	1	0	0	0	1	0	0	0	0	0	0	0	0	0	0
2	0	1	1	0	0	1	0	0	0	0	0	0	0	0	0	0	0
3	0	0	1	0	0	0	0	0	0	0	0	0	0	0	0	0	0
4	0	0	1	1	0	1	0	0	0	0	0	0	0	0	0	0	0
5	0	0	0	0	1	0	0	1	0	0	1	0	0	0	0	0	0
6	0	0	0	0	0	1	0	0	0	0	0	0	1	0	0	0	0
7	0	0	0	0	0	1	1	1	0	0	0	0	0	0	0	0	0
8	0	0	0	0	0	1	0	1	0	1	0	0	0	0	0	0	0
9	0	0	0	1	0	1	0	0	1	0	0	0	0	0	0	0	0
10	0	0	0	0	0	0	0	0	0	1	1	0	0	0	0	0	0
11	0	0	0	0	0	0	0	0	0	0	1	1	1	1	0	0	0
12	0	0	0	0	0	0	0	0	0	0	0	1	1	0	0	0	0
13	0	0	0	0	0	0	0	0	0	0	0	1	1	0	1	1	0
14	0	0	0	0	0	1	0	0	0	0	0	0	0	1	0	0	0
15	0	1	1	0	0	0	0	0	0	0	0	0	0	0	1	0	0
16	0	0	0	0	0	0	0	0	0	0	0	0	1	0	1	1	0
17	1	0	0	0	0	0	0	0	0	0	0	0	0	0	0	0	1

Table 5
Reachability matrix **RE**

	1	2	3	4	5	6	7	8	9	10	11	12	13	14	15	16	17
1	1	1	1	0	0	1	0	0	0	0	0	0	0	1	0	0	0
2	0	1	1	0	0	1	0	0	0	0	0	0	0	1	0	0	0
3	0	0	1	0	0	0	0	0	0	0	0	0	0	0	0	0	0
4	0	0	1	1	0	1	0	0	0	0	0	0	0	1	0	0	0
5	0	1	1	0	1	1	0	1	0	1	1	1	1	1	1	1	0
6	0	0	0	0	0	1	0	0	0	0	0	0	0	1	0	0	0
7	0	0	0	0	0	1	1	0	0	0	0	0	0	1	0	0	0
8	0	1	1	0	0	1	0	1	0	1	1	1	1	1	1	1	0
9	0	0	1	1	0	1	0	0	1	0	0	0	0	1	0	0	0
10	0	1	1	0	0	1	0	0	0	1	1	1	1	1	1	1	0
11	0	1	1	0	0	1	0	0	0	1	1	1	1	1	1	1	0
12	0	1	1	0	0	1	0	0	0	0	0	1	1	1	1	1	0
13	0	1	1	0	0	1	0	0	0	0	0	1	1	1	1	1	0
14	0	0	0	0	0	1	0	0	0	0	0	0	0	1	0	0	0
15	0	1	1	0	0	1	0	0	0	0	0	0	0	1	1	0	0
16	0	1	1	0	0	1	0	0	0	0	0	1	1	1	1	1	0
17	1	1	1	0	0	1	0	0	0	0	0	0	0	1	0	0	1

Table 6
ISM of TE process

Level	Small control loop set
Level 1	3, 6, 14
Level 2	2, 4, 7
Level 3	1, 9, 15
Level 4	12, 13, 16, 17
Level 5	10, 11
Level 6	8
Level 7	5

the fault point. The abscissa of the first crest is 48, which can be converted to time point $48 \times 64 \times 0.01 = 30.72$ h. Because the length of window is 4096, the fault point can be calculated as $30.72 + 4096 \times 0.01 = 71.68$ h. This method can detect not only the fault loop 7 but also the fault point. The proposed method shows higher output level and higher recognition rate. In other words, the method is more sensitive in detecting small changes in control loops and demonstrates persistent fault detection.

4.3.2. Case 2—IDV(11)

IDV(11) (random signal), the inlet temperature of cooling water is interfered at 55 h and eliminated at 151 h.

As shown by loop 7 in Fig. 5, the fault point is located with the first crest moving 64 along the abscissa direction. The fault eliminate point is at the second crest.

For NLI, it has a step change when the fault signal enters the window of 4096, and its value increases suddenly; it falls to ultimate stability as the fault signal moves along the window and the proportion of fault

data increases in the window, but it is larger than that in normal situation; it rises as the proportion of fault data reduces, and its value reaches the maximum with a small amount of data; it returns to a steady state gradually with normal signal only because the fault signal moves out of the window.

The abscissa of the first crest is 26, which is converted to time point as $26 \times 64 \times 0.01 = 16.64$ h, and the fault point is $16.64 + 64 \times 64 \times 0.01 = 57.6$ h. The abscissa of the second crest is 237, fault elimination point is at $237 \times 64 \times 0.01 = 151.68$ h. It is consistent with that under the actual situation. This method can detect both the location of fault and the fault point and elimination point.

4.3.3. Case 3—IDV(14)

IDV(14), sticking of reactor cooling water valve, is interfered at 55 h and eliminated at 130 h.

As shown by loop 7 in Fig. 6, the fault point is in the location of the first crest moving 64 along abscissa direction. The fault elimination point is in the second crest. This figure is similar to Fig. 5. The abscissa of the first crest is 22 and is converted to time point $22 \times 64 \times 0.01 = 14.08$ h, and the fault point is at $14.08 + 4096 \times 0.01 = 55.04$ h. The abscissa of the second crest is 202, and the fault elimination point is at $202 \times 64 \times 0.01 = 129.28$ h.

4.3.4. Case 4—IDV(12)

IDV(12), condenser cooling water inlet temperature, is interfered at 56 h and eliminated at 143 h. After this small control loop set (loop 8) of Level 6 (Table 6) is used to index calculation, this fault is detected. Only indexes of loops 5 and 8 need to be calculated. The result is showed in Fig. 7. For NLI, the abscissa of the first crest is 25, with time point at $25 \times 64 \times 0.01 = 16$ h and the fault point at $16 + 64 \times 64 \times 0.01 = 56.96$ h. The abscissa of the second crest is 223, and the fault elimination point is at $223 \times 64 \times 0.01 = 142.72$ h. We can also obtain the fault point and eliminate the fault, but this case is not as clear as the previous three cases, because of lower changes of the control loop variables after the fault occurs.

The faults in the four cases can be detected and their locations are determined. The proposed method reduces the number of control loops or variables with interpretative structural for large-scale process control system and cuts off the amount of calculation when the process is a large-scale one such as TE. It should be noted that PCA-based method [32], such as HOS, is a data-driven method and belongs to those based on signal processing. Both methods are applicable to fault detection of linear and nonlinear systems. However, the methods for fault detection and fault isolation are not satisfactory. A combination with other theoretical methods is needed in order to improve the performance of fault detection and diagnosis [33].

Table 7 shows the features of the methods introduced in this paper as well as the traditional method for large-scale control system. HOS is usually used in the diagnosis and detection of large-scale control systems, with large amount of calculation and higher cost. In order to
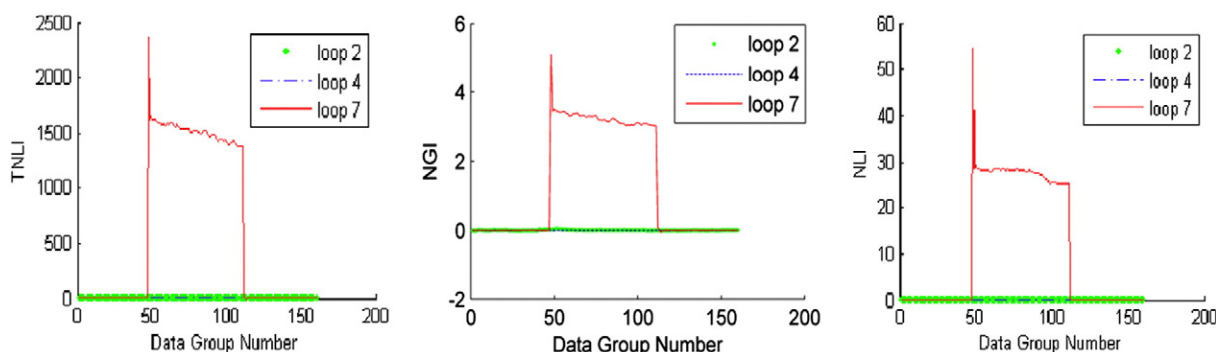

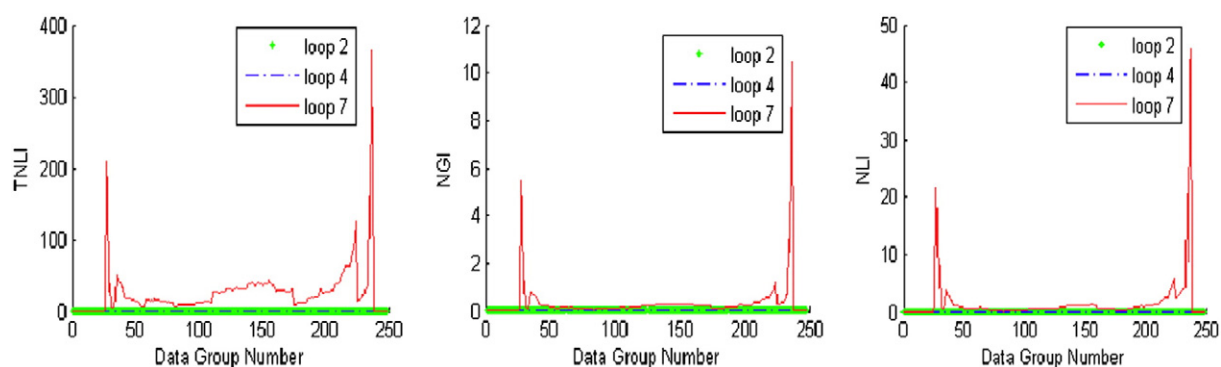**Fig. 4.** TNLI, NGI and NLI of loops 2, 4 and 7 with IDV(4).

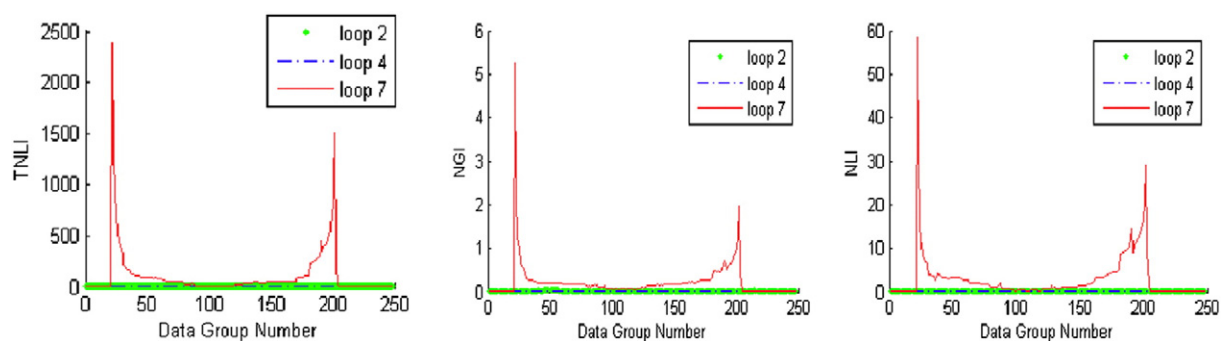Fig. 5. TNLI, NGI and NLI of loops 2, 4 and 7 with IDV(11).

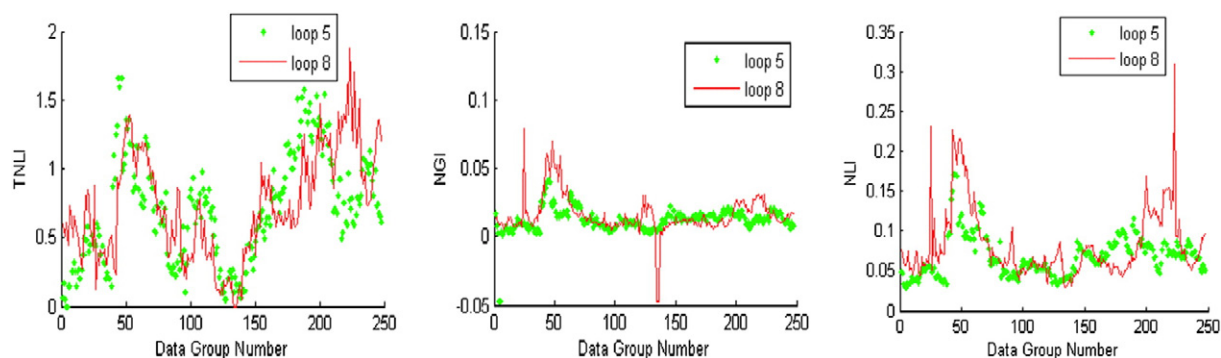Fig. 6. TNLI, NGI, NLI of loops 2, 4 and 7 with IDV(14).

Fig. 7. TNLI, NGI, NLI of loops 5 and 8 with IDV(12).

Table 7
The features of the methods cited in this paper

Method	Characteristics
HOS	① Good effect on non-Gaussian and nonlinear signal detection and suitable to nonlinear and non-Gaussian feature extraction and diagnosis
	② Large calculation cost for large-scale process control systems, inefficiency and blindness, difficult to judge fault location
ISM	① Vague ideas in well-structured and intuitive relationship model, applicable to a number of variables, relationships, and complex system analysis
	② Using prior knowledge, inaccurate and inefficient lacking of prior knowledge
ISM based on partial correlation coefficient	① With partial correlation coefficient and prior knowledge to improve the accuracy of traditional ISM
	② With advantages of ISM
ISM-HOS	① With advantages of HOS for non-Gaussian and nonlinear signal detection and advantages of ISM
	② Enhancing efficiency of detection and diagnosis, reducing calculation cost
	③ Much easier fault location than HOS
	④ Difficult to detect fault without significant change of nonlinear characteristics of control loop
PCA-based	① Good effect on detection for linear Gaussian signal, used for linear Gaussian feature extraction and diagnosis
	② Large amount of calculation and higher cost for large-scale process control system, not very ideal for fault detection and diagnosis
	③ Improving diagnosis efficiency combined with other theories such as neural network

improve the efficiency of diagnosis, ISM is introduced and modified to a new method, ISM based on partial correlation coefficient. In addition, we combine it with *a priori* knowledge to improve the accuracy of traditional ISM, especially for a large-scale control system. The combination of HOS and ISM improves the efficiency and avoids the blindness of HOS detection.

5. Conclusions

The presented HOS–ISM based fault diagnosis framework integrates HOS and ISM and combines *a priori* process with data-driven methods to determine control loop, increase the accuracy of data selection, and cover the shortage of uncertainty in diagnosis result of HOS due to the selection of different data sets. The calculation of nonlinear index online, its dynamic changes, intuitive identification of the fault loop, determination and elimination of the fault point all have important practical significance. However, without a significant change of nonlinear characteristics of the control loop, detection of fault is difficult, which will be improved in the further work.

References

[1] V. Venkatasubramanian, R. Rengaswamy, K. Yin, S.N. Kavuri, A review of process fault detection and diagnosis (Part I): Quantitative model-based methods, *Comput. Chem. Eng.* 27 (3) (2003) 293–311.
[2] V. Venkatasubramanian, R. Rengaswamy, K. Yin, S.N. Kavuri, A review of process fault detection and diagnosis (Part II): Qualitative models and search strategies, *Comput. Chem. Eng.* 27 (3) (2003) 313–326.
[3] V. Venkatasubramanian, R. Rengaswamy, K. Yin, S.N. Kavuri, A review of process fault detection and diagnosis (part III): Process history based methods, *Comput. Chem. Eng.* 27 (3) (2003) 327–346.
[4] Fu. Kechang, Wu. Tiejun, Feature subspace based KPCA and its application to fault detection and diagnosis, *J. Chem. Ind. Eng.* 57 (11) (2006) 2664–2669.
[5] Zhang Yingwei, Ma Chi, Fault diagnosis of nonlinear processes using multi-scaleKPCA and multi-scale KPLS, *Chem. Eng. Sci.* 66 (1) (2011) 64–72.
[6] Chen Xinyi, Yan Xuefeng, Fault diagnosis in chemical process based on self-organizing map integrated with fisher discriminant analysis, *Chin. J. Chem. Eng.* 21 (4) (2013) 382–387.
[7] P.M. Frank, New developments using AI in fault diagnosis, *Eng. Appl. Artif. Intell.* 10 (1) (1997) 3–14.
[8] R.J. Patton, C.J. Lopez-Toribio, F.J. Uppal, Artificial intelligence approaches to fault diagnosis for dynamical systems, *Int. J. Appl. Math. Comput. Sci.* 9 (3) (1999) 471–518.
[9] M.A. Hussain, C.R. Che Hassan, K.S. Loh, K.W. Mah, Application of artificial intelligence technique in process fault diagnosis, *J. Eng. Sci. Technol.* 2 (3) (2007) 260–270.
[10] Jin Xin, Ren Xianbin, Zhou Liang, Overview on intelligent technology of fault diagnosis, *Foreign Electron. Meas. Technol.* 28 (7) (2009) 30–32.
[11] Y.C. Kim, E.J. Powers, Digital bispectral analysis and its applications to nonlinear wave interactions, *IEEE Trans. Plasma Sci.* 7 (2) (1979) 120–131.
[12] C.L. Nikias, A. Petropulu, Higher-order Spectra: A Nonlinear Signal Processing Frame Work, Prentice-Hall, Englewood CliWs, N.J., 1993.
[13] J.W.A. Fackrell, Bispectral Analysis of Speech Signals, The University of Edinburgh, UK, 1996. (Ph.D.Thesis).
[14] M.A.A. Shoukat Choudhury, Sirish.L. Shah, Nina.F. Thornhillb, Diagnosis of poor control-loop performance using higher-order statistics, *Automatica* 40 (10) (2004) 1719–1728.
[15] M.A.A. Shoukat Choudhury, Troubleshooting plant wide oscillations using nonlinearity information, *J. Chem. Eng.* 24 (1) (2006) 50–60.
[16] Peng Danlin, Study on interpretative structural modeling and its application to summarized design, *Eng. J. Wuhan Univ.* 39 (1) (2006) 137–142.
[17] W.U. Wang Conglu, L.I. Shuqing Chao, Layer analysis of accident causes based on-interpretation structure model, *MINING R & D* 24 (5) (2004) 77–79.
[18] Tian Yanqing, Yang Zhenhong, Li Hua, S.H.A.N.G. Xuguang, Study on affecting factors of risks at workplace based on ISM and AH, *China Saf. Sci. J.* 21 (1) (2011) 140–146.
[19] M.D. Singh, R. Kant, Knowledge management barriers: an interpretive structural modeling approach, Industrial Engineering and Engineering Management, 2007 IEEE International Conference on Date of Conference, 2007, pp. 2091–2095.
[20] Yan Likun, Application of correlation coefficient and biased correlation coefficient in related analysis, *J. Yunnan Univ. Finance Econ.* 19 (3) (2003) 78–80.
[21] Wang Haiyan, Yang Fangting, Liu Lu, Comparison and application of standardized regressive coefficient & partial correlation coefficient, *Journal of Quantitative & Technical Economics* (2006) 150–155.
[22] Jong-Min Kim, Yoon-Sung Jung, Taeryon Choi, Engin A. Sungura, Partial correlation with copula modeling, *Computational Statistics and Data Analysis* 55 (3) (2011) 1357–1366.
[23] Yang Fan, Member, SirishL. Shah, Deyun Xiao, Signed directed graph modeling of industrial processes and their validation by data-based methods, 2010 Conference on. IEEE, 2010, pp. 387–392.
[24] Jiang Hailei, Rohit Patwarhan, Sirish L. Shah, Root cause diagnosis of plant-wideoscillations using the concept of adjacency matrix, *J. Process Control* 19 (8) (2009) 1347–1354.
[25] N.F. Thornhill, A. Horch, Advances and new directions in plant-wide disturbance detection and diagnosis, *Control. Eng. Pract.* 15 (10) (2007) 1196–1206.
[26] J.J. Downs, E.F. Vogel, A plant-wide industrial process control problem, *Comput. Chem. Eng.* 17 (3) (1993) 245–255.
[27] Xu. Peng Di, Zhu Qunxiong Yuan, Study and application of case-based extension fault diagnosis for chemical process, *Chin. J. Chem. Eng.* 21 (4) (2013) 366–375.
[28] Xie Xiang, Shi Hongbo, Multimode process monitoring based on fuzzy C-means in locality preserving projection subspace, *Chin. J. Chem. Eng.* 20 (6) (2012) 1174–1179.
[29] Song Kai, L.I. Wang Haiqing, F.E.N.G. Zhigang Ping, Quality based prioritized sensor fault monitoring methodology, *Chin. J. Chem. Eng.* 16 (4) (2008) 584–589.
[30] M. Golshan, R. Bozorgmehry boozarjomehry, M.R. Pishvaie, A new approach to real time optimization of the Tennessee Eastman challenge problem, *Chem. Eng. J.* 112 (2005) 33–44.
[31] Truls Larsson, Self-optimizing control of a large-scale plant: the Tennessee Eastman, process, *Ind. Eng. Chem. Res.* 40 (22) (2001) 4889–4901.
[32] Shen Yina, Steven X. Ding, A comparison study of basic data-driven fault diagnosis and process monitoring methods on the benchmark Tennessee Eastman process, *J. Process Control* 22 (9) (2012) 1567–1581.
[33] Zhang Ailing, Zhang Wenying, Zhang Duanjin, Survey on fault detection and diagnosis for control systems, *Systems Engineering and Electronics* 29 (4) (2007) 659–664.